

Synthesis of densely functionalized chromenes using a magnetic recoverable ionic liquid as the catalyst

Forough Ramezanzadeh^a, Manouchehr Mamaghani^{b,*}, Hossein Fallah-Bagher Shaidaei^a, Mehdi Sheykhani^b

a) Department of Chemistry, Faculty of Sciences, Islamic Azad University, Rasht Branch, Rasht, Iran

b) Department of Chemistry, Faculty of Sciences, University of Guilan, P.O. Box 41335-1914, Rasht, Iran

Received 27 December 2019; received in revised form 10 September 2020; accepted 14 September 2020

ABSTRACT

In the present study, robust, versatile and straightforward strategy for the diversity-oriented convergent synthesis of a vast range of highly functionalized and biologically effective chromenes is introduced with the reaction of malononitrile, dimedone/cyclohexadione/4-hydroxycoumarin and benzaldehydes in the presence of $[\gamma\text{-Fe}_2\text{O}_3\text{@HAp-Si}(\text{CH}_2)_3\text{BF}_4\text{@DMIM}]$ as the catalyst. The structures of all the newly synthesized products were characterized by spectroscopic (FT-IR, ^1H NMR, ^{13}C NMR) and elemental analyses. This method benefits from several advantages such as using easily recoverable magnetic nanocatalyst, simple work up, short reaction time and excellent yields. The prepared nanoparticles were fully characterized by various spectroscopic, thermal and magnetic analyses. The catalyst exhibited good reusability feature and no loss of activity was observed even after 8 successive runs.

Keywords: Benzopyran, Chromene, $\gamma\text{-Fe}_2\text{O}_3$, HAp, Magnetic Nanocatalyst, Ionic Liquid.

1. Introduction

In recent years, the use of multicomponent reactions to synthesize heterocyclic compounds has been of great interest to researchers. Due to the importance of chromene motifs as oxygen-containing heterocycles in the synthesis of pharmaceuticals, considerable attention has been directed towards the synthesis of these structures [1]. Many reports have been disclosed concerning biological properties of chromenes and benzochromenes, such as anticancer [2], anti-HIV-1 [3], anti-inflammatory [4], antioxidant [5], anti-alzheimer [6] antimicrobial [7], in vitro antibacterial, MRSA and antifungal [8]. Also, in this respect, recently Ablewi and coworkers reported the synthesis of some benzochromenes having significant anti-cancer features [9]. Thus, because of impressive biological activities of chromene derivatives, various numbers of chemical methods have been reported for their synthesis using various catalysts such as basic conditions [10], modified

halloysite nanotubes [11], tantalum mesoporous silicas [12], KF grafted on clinoptilolite [13], nickel ferrite [14], alumina-supported cobalt [15], nano-kaoline/BF₃/Fe₃O₄ [16], Fe₃O₄ [17], oxovanadium(IV) complex supported on the surface of modified Fe₃O₄ with a silica shell [18], and 4-aminiquinaldine loaded on Fe₃O₄@SiO₂ [19].

Due to leading performance of nanoparticles in the synthesis of organic compounds for having high surface area, recoverability, facile workup and separation [20-23]. In continuation of our previous works [24-27] we introduce $[\gamma\text{-Fe}_2\text{O}_3\text{@HAp-Si}(\text{CH}_2)_3\text{BF}_4\text{@DMIM}]$ MNPs as novel, recoverable, and stable catalysts for the preparation of chromene derivatives with numerous synthetic applications.

2. Experimental

2.1. General

Electrothermal 9100 apparatus was used for melting points determination and Shimadzo IR-470 spectrometer was applied for IR spectra. ^1H and ^{13}C NMR spectra were recorded by a 400 MHz Bruker

*Corresponding author:

E-mail address: *m-chem41@guilan.ac.ir; mchem41@gmail.com*
(M. Mamaghani)

DRX-400 in deuterated DMSO using TMS as an internal standard. X-ray powder diffraction was recorded with a Philips X-Pert MPD diffractometer using a Cobalt tube. Philips XL30 electron microscope was used for SEM images. Elemental analysis was done on a Carlo-Erba EA1110 CNNO-S analyzer and confirmed by the calculated values. All chemicals were obtained from Merck and used without further purification. All solvents used were dried and distilled according to standard procedures. Scanning electron microphotographs (SEM-EDX) were recorded by using a PHILIPS XL30 electron microscope. Vibrating sample magnetometer was used to determine magnetic properties of the catalyst.

2.2. Preparation of $[\gamma\text{-Fe}_2\text{O}_3@\text{HAp-Si}(\text{CH}_2)_3\text{BF}_4@\text{DMIM}] \text{ MNPs (5)}$

$[\gamma\text{-Fe}_2\text{O}_3@\text{HAp}]$ and $[\gamma\text{-Fe}_2\text{O}_3@\text{HAp-Si}(\text{CH}_2)_3\text{Cl}]$ were prepared based on the literature [28-31]. 1,2-Dimethylimidazole (53 mmol) was refluxed in 50 mL toluene for 12 h under Ar in the presence of $[\gamma\text{-Fe}_2\text{O}_3@\text{HAp-Si}(\text{CH}_2)_3\text{Cl}]$. The magnetic nanoparticles thus obtained, were separated via a magnetic device. Having washed with toluene, the mixture was then dried at 120 °C to furnish catalyst **4** (96% yield). In the next step, to a solution of synthesized nanocatalyst in 10 mL water, 3 mmol NaBF_4 was added. After stirring for 5 h, the solid was washed several times with distilled water to remove the produced sodium chloride.

2.3. Typical method for the synthesis of chromenes

1 mmol of malononitrile was mixed with dimedone/cyclohexadione/4-hydroxycoumarin (1 mmol) and benzaldehydes (1 mmol) in 10 mL EtOH and then the prepared catalyst **5** (0.02 g) was added and the reaction was conducted at 80 °C for the requisite reaction time (**Table 4**). When the reaction completed (monitored by thin-layer chromatography), the catalyst separated via an external magnet. After adding distilled water to the resultant solution, the mixture was then filtered. As the final step, recrystallization from EtOH led to the desired product which was characterized by spectroscopic methods (**11-13**) (**Table 4, Fig. 8**).

2.4. Some Representative Spectral data (Table 4):

2.4.1. 2-Amino-4-(3-methylphenyl)-3-cyano-7,7-dimethyl-5-oxo-4H-5,6,7,8-tetrahydrobenzo-pyran (11a). Melting point: 198-200 °C. FT-IR (KBr, ν , cm^{-1}): 3350, 3258, 3177 (NH_2), 2191 (cyano group), 1684 (carbonyl group), 1655 (olefinic bond), 1370 (C-H bend, Me), 1214, 1034 (C-O). ^1H NMR (400 MHz, DMSO- d_6 , δ , ppm): 7.19 (t, 1H, $J = 7.4$ Hz, Ar-H), 7.03

(s, 2H, NH_2), 7.00-6.93 (m, 3H, Ar-H), 4.14 (s, 1H, CH), 2.59-2.49 (m, 2H, $\text{CH}_2\text{-C=O}$), 2.29 (s, 3H, Me), 2.27, 2.12 (d, 2H, $J = 16.0$ Hz, $\text{CH}_2\text{-C}$), 1.06 (s, 3H, Me), 0.98 (s, 3H, Me). ^{13}C NMR (100 MHz, DMSO- d_6 , δ , ppm): 196.2, 162.9, 158.9, 145.2, 137.8, 128.7, 128.2, 127.8, 124.8, 120.3, 113.2, 58.8, 50.4, 36.0, 32.3, 28.9, 27.2, 21.6. Anal. calcd for $\text{C}_{19}\text{H}_{20}\text{N}_2\text{O}_2$ (308.37): C, 74.00; H, 6.54; N, 9.09; found: C, 74.15; H, 6.43; N, 9.20%.

2.4.2. 2-Amino-4-(2-fluorophenyl)-3-cyano-7,7-dimethyl-5-oxo-4H-5,6,7,8-tetrahydrobenzo-pyran (11b). Melting point: 250-251 °C. FT-IR (KBr, ν , cm^{-1}): 3398, 3328, 3212 (NH_2), 2198 (cyano group), 1682 (carbonyl group), 1658 (olefinic bond), 1370 (C-H bend, Me), 1215, 1037 (C-O), 1160 (C-F). ^1H NMR (400 MHz, DMSO- d_6 , δ , ppm): 7.27-7.11 (m, 4H, Ar-H), 7.08 (br. s, 2H, NH_2), 4.47 (s, 1H, CH), 2.58, 2.48 (ABq, $J = 17.4$ Hz, 2H, $\text{CH}_2\text{-C=O}$), 2.29, 2.11 (ABq, $J = 16.0$ Hz, 2H, $\text{CH}_2\text{-C}$), 1.06 (s, 3H, Me), 0.98 (s, 3H, Me). ^{13}C NMR (100 MHz, DMSO- d_6 , δ , ppm): 196.1, 163.6, 160.4 (d, $^1\text{J}_{\text{C-F}} = 241.0$ Hz), 131.8, 131.6, 130.2 (d, $^4\text{J}_{\text{C-F}} = 3.0$ Hz), 129.1 (d, $^3\text{J}_{\text{C-F}} = 8.0$ Hz), 124.9, 120.0, 115.9 (d, $^2\text{J}_{\text{C-F}} = 22.0$ Hz), 111.8, 57.1, 50.4, 32.3, 30.3, 29.0, 27.1, 19.0. Anal. calcd for $\text{C}_{18}\text{H}_{17}\text{FN}_2\text{O}_2$ (312.34): C, 69.22; H, 5.49; N, 8.97; found: C, 69.05; H, 5.36; N, 8.79%.

2.4.3. 2-Amino-4-(2-chlorophenyl)-3-cyano-7,7-dimethyl-5-oxo-4H-5,6,7,8-tetrahydrobenzo-pyran (11c). Melting point: 213-215 °C. FT-IR (KBr, ν , cm^{-1}): 3389, 3327, 3255 (NH_2), 2198 (cyano group), 1681 (carbonyl group), 1658 (olefinic bond), 1369 (C-H bend, Me), 1215 (C-O), 1038 (C-Cl). ^1H NMR (400 MHz, DMSO- d_6 , δ , ppm): 7.39 (dd, 1H, $J = 7.6, 1.2$ Hz, Ar-H), 7.30 (td, $J = 7.2, 1.3$ Hz, 1H, Ar-H), 7.23 (dd, 1H, $J = 7.6, 2.0$ Hz, Ar-H), 7.21-7.17 (m, 1H, Ar-H), 7.08 (br. s, 2H, NH_2), 4.71 (s, 1H, CH), 2.58, 2.48 (ABq, $J = 17.4$ Hz, 2H, $\text{CH}_2\text{-C=O}$), 2.27, 2.10 (d, 2H, $J = 16.0$ Hz, $\text{CH}_2\text{-C}$), 1.06 (s, 3H, Me), 1.00 (s, 3H, Me). ^{13}C NMR (100 MHz, DMSO- d_6 , δ , ppm): 196.1, 163.6, 159.1, 142.0, 132.6, 130.4, 129.9, 128.7, 127.9, 119.8, 112.2, 57.2, 50.4, 33.3, 32.3, 28.9, 27.3, 19.0. Anal. calcd for $\text{C}_{18}\text{H}_{17}\text{ClN}_2\text{O}_2$ (328.79): C, 65.75; H, 5.21; N, 8.52; found: C, 65.63; H, 5.06; N, 8.39%.

2.4.4. 2-Amino-4-(2-methoxyphenyl)-3-cyano-7,7-dimethyl-5-oxo-4H-5,6,7,8-tetrahydrobenzo-pyran (11d). Melting point: 202-204 °C. FT-IR (KBr, ν , cm^{-1}): 3395, 3329, 3219 (NH_2), 2189 (cyano group), 1688 (carbonyl group), 1654 (olefinic bond), 1372 (C-H bend, Me), 1248, 1213, 1014 (C-O). ^1H NMR (400 MHz, DMSO- d_6 , δ , ppm): 7.19 (t, 1H, $J = 7.4$ Hz, Ar-H), 7.03 (d, 1H, $J = 7.2$ Hz, Ar-H), 6.98 (d, 1H, $J = 8.0$ Hz, Ar-H), 6.89-6.87 (m, 1H, Ar-H), 6.87 (s, 2H, NH_2), 4.52 (s, 1H, CH), 3.78 (s, 3H, OCH_3), 2.58, 2.48 (ABq,

$J = 17.6$ Hz, 2H, $\text{CH}_2\text{-C=O}$), 2.28, 2.09 (ABq, 2H, $J = 16.4$ Hz, $\text{CH}_2\text{-C}$), 1.07 (s, 3H, Me), 0.99 (s, 3H, Me). ^{13}C NMR (100 MHz, DMSO-d_6 , δ , ppm): 196.1, 163.6, 159.5, 157.3, 132.6, 129.0, 128.3, 120.8, 120.4, 112.4, 111.9, 57.8, 56.1, 50.5, 32.3, 30.8, 29.1, 27.0. Anal. calcd for $\text{C}_{19}\text{H}_{20}\text{N}_2\text{O}_3$ (324.37): C, 70.35; H, 6.21; N, 8.64; found: C, 70.21; H, 6.12; N, 8.51%.

2.4.5. 2-Amino-4-(2-methoxyphenyl)-3-cyano-5-oxo-4H-5,6,7,8-tetrahydrobenzo-pyran (12a).

Melting point: 193-194 °C. FT-IR (KBr, ν , cm^{-1}): 3447, 3320, 3176 (NH_2), 2198 (cyano group), 1682 (carbonyl group), 1648 (olefinic bond), 1368 (C-H bend, Me), 1252, 1207, 1065 (C-O). ^1H NMR (400 MHz, DMSO-d_6 , δ , ppm): 7.18 (t, 1H, $J = 7.6$ Hz, Ar-H), 7.01-6.97 (m, 2H, Ar-H), 6.89-6.85 (m, 3H, NH_2 , Ar-H), 4.57 (s, 1H, CH), 3.79 (s, 3H, OCH_3), 2.64 (br. s, 2H, $\text{CH}_2\text{-C=O}$), 2.32-2.22 (m, 2H, $\text{CH}_2\text{-C=C}$), 1.99-1.94 (m, 2H, CH_2). ^{13}C NMR (100 MHz, DMSO-d_6 , δ , ppm): 196.3, 165.6, 159.4, 157.2, 133.0, 128.5, 128.2, 121.0, 120.3, 113.6, 112.0, 58.0, 56.2, 36.9, 30.0, 27.0, 20.4. Anal. calcd for $\text{C}_{17}\text{H}_{16}\text{N}_2\text{O}_3$ (296.32): C, 68.91; H, 5.44; N, 9.45; found: C, 68.78; H, 5.32; N, 9.31%.

2.4.6. 2-Amino-4-(2-bromophenyl)-3-cyano-5-oxo-4H-5,6,7,8-tetrahydrobenzo-pyran (12b).

Melting point: 194-196 °C. FT-IR (KBr, ν , cm^{-1}): 3474, 3314, 3175 (NH_2), 2187 (cyano group), 1682 (carbonyl group), 1657 (olefinic bond), 1247 (C-O), 1021 (C-Br). ^1H NMR (400 MHz, DMSO-d_6 , δ , ppm): 7.55 (d, 1H, $J = 8.0$ Hz, Ar-H), 7.32 (t, 1H, $J = 7.4$ Hz, Ar-H), 7.18 (d, 1H, $J = 7.6$ Hz, Ar-H), 7.14 (t, 1H, $J = 7.6$ Hz, Ar-H), 7.06 (br. s, 2H, NH_2), 2.69-2.65 (m, 2H, $\text{CH}_2\text{-C=O}$), 2.34-2.20 (m, 2H, $\text{CH}_2\text{-C=C}$), 1.99-1.94 (m, 2H, CH_2). ^{13}C NMR (100 MHz, DMSO-d_6 , δ , ppm): 196.2, 165.5, 158.9, 144.0, 133.0, 130.3, 128.9, 128.6, 123.2, 119.7, 113.6, 57.5, 36.8, 35.4, 27.0, 20.3. Anal. calcd for $\text{C}_{16}\text{H}_{13}\text{BrN}_2\text{O}_2$ (345.19): C, 55.67; H, 3.80; N, 8.12; found: C, 55.54; H, 3.92; N, 8.24%.

2.4.7. 2-Amino-4-(2-fluorophenyl)-3-cyano-5-oxo-4H-5,6,7,8-tetrahydrobenzo-pyran (12c).

Melting point: 252-253 °C. FT-IR (KBr, ν , cm^{-1}): 3324, 3175 (NH_2), 2191 (cyano group), 1686 (carbonyl group), 1647 (olefinic bond), 1257, 1210 (C-O), 1166 (C-F). ^1H NMR (400 MHz, DMSO-d_6 , δ , ppm): 7.28-7.21 (m, 1H, Ar-H), 7.19 (d, 1H, $J = 7.2$ Hz, Ar-H), 7.15-7.10 (m, 2H, Ar-H), 7.07 (br. s, 2H, NH_2), 4.50 (s, 1H, CH), 2.64 (br. s, 2H, $\text{CH}_2\text{-C=O}$), 2.37-2.22 (m, 2H, $\text{CH}_2\text{-C=C}$), 2.02-2.00 (m, 2H, CH_2). ^{13}C NMR (100 MHz, DMSO-d_6 , δ , ppm): 196.3, 165.6, 160.3 (d, $^1\text{J}_{\text{C-F}} = 244.0$ Hz), 131.9, 131.8, 130.0 (d, $^4\text{J}_{\text{C-F}} = 4.0$ Hz), 129.0 (d, $^3\text{J}_{\text{C-F}} = 8.0$ Hz), 125.0, 120.0, 115.8 (d, $^2\text{J}_{\text{C-F}} = 22.0$ Hz), 112.9, 57.2, 36.7, 29.9, 27.0, 20.3. Anal. calcd for $\text{C}_{16}\text{H}_{13}\text{FN}_2\text{O}_2$ (284.29): C, 67.60; H, 4.61; N, 9.85; found: C, 67.44; H, 4.72; N, 9.97%.

C=C), 2.02-2.00 (m, 2H, CH_2). ^{13}C NMR (100 MHz, DMSO-d_6 , δ , ppm): 196.3, 165.6, 160.3 (d, $^1\text{J}_{\text{C-F}} = 244.0$ Hz), 131.9, 131.8, 130.0 (d, $^4\text{J}_{\text{C-F}} = 4.0$ Hz), 129.0 (d, $^3\text{J}_{\text{C-F}} = 8.0$ Hz), 125.0, 120.0, 115.8 (d, $^2\text{J}_{\text{C-F}} = 22.0$ Hz), 112.9, 57.2, 36.7, 29.9, 27.0, 20.3. Anal. calcd for $\text{C}_{16}\text{H}_{13}\text{FN}_2\text{O}_2$ (284.29): C, 67.60; H, 4.61; N, 9.85; found: C, 67.44; H, 4.72; N, 9.97%.

2.4.8. 2-Amino-4-(3-methylphenyl)-3-cyano-5-oxo-4H-5,6,7,8-tetrahydrobenzo-pyran (12d).

Melting point: 220-221 °C. FT-IR (KBr, ν , cm^{-1}): 3313, 3160 (NH_2), 2194 (cyano group), 1684 (carbonyl group), 1647 (olefinic bond), 1366 (C-H bend, Me), 1252, 1207 (C-O). ^1H NMR (400 MHz, DMSO-d_6 , δ , ppm): 7.19 (t, 1H, $J = 7.4$ Hz, Ar-H), 7.02-6.97 (m, 5H, NH_2 , Ar-H), 4.18 (s, 1H, CH), 2.64-2.60 (m, 2H, $\text{CH}_2\text{-C=O}$), 2.33-2.29 (m, 5H, $\text{CH}_2\text{-C=C}$, CH_3), 2.00-1.90 (m, 2H, CH_2). ^{13}C NMR (100 MHz, DMSO-d_6 , δ , ppm): 196.4, 164.9, 159.0, 145.2, 137.8, 128.7, 128.2, 127.7, 124.8, 120.3, 114.3, 58.7, 36.8, 35.8, 27.0, 21.6, 20.3. Anal. calcd for $\text{C}_{17}\text{H}_{16}\text{N}_2\text{O}_2$ (280.32): C, 72.84; H, 5.75; N, 9.99; found: C, 72.95; H, 5.63; N, 9.83%.

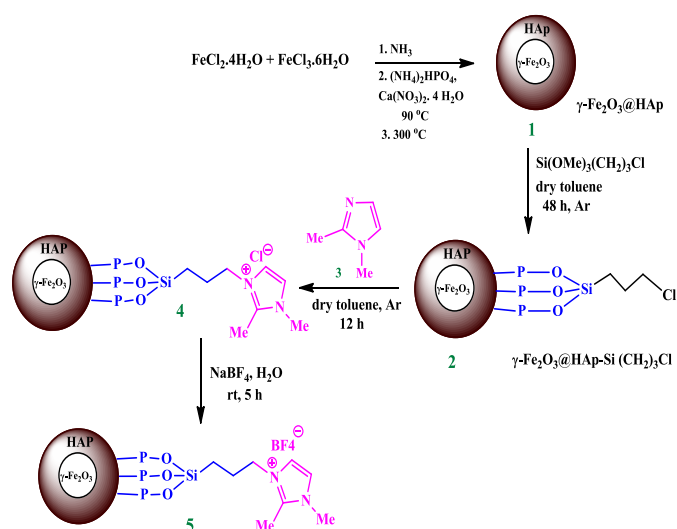
2.4.9. 2-Amino-4-(4-hydroxy-3-methoxyphenyl)-3-cyano-5-oxo-4H-5,6,7,8-tetrahydrobenzo-pyran (12e).

Melting point: 239-241 °C. FT-IR (KBr, ν , cm^{-1}): 3422, 3325, 3266 (NH_2 , OH), 2193 (cyano group), 1674 (carbonyl group), 1635 (olefinic bond), 1367 (C-H bend, Me), 1246, 1204, 1030 (C-O). ^1H NMR (400 MHz, DMSO-d_6 , δ , ppm): 8.85 (s, 1H, OH), 6.96 (br. s, 2H, NH_2), 6.71-6.69 (m, 2H, Ar-H), 6.54 (d, 1H, $J = 8.0$ Hz, Ar-H), 4.13 (s, 1H, CH), 3.76 (s, 3H, OCH_3), 2.63 (br. s, 2H, $\text{CH}_2\text{-C=O}$), 2.30 (br. s, 2H, $\text{CH}_2\text{-C=C}$), 1.97-1.91 (m, 2H, CH_2). ^{13}C NMR (100 MHz, DMSO-d_6 , δ , ppm): 196.4, 164.6, 158.9, 147.7, 145.7, 136.3, 120.5, 119.7, 115.8, 114.6, 112.0, 59.0, 56.0, 36.9, 35.3, 27.0, 20.3. Anal. calcd for $\text{C}_{17}\text{H}_{16}\text{N}_2\text{O}_4$ (312.32): C, 65.38; H, 5.16; N, 8.97; found: C, 65.25; H, 5.02; N, 8.81%.

3. Results and Discussion

3.1. Preparation of the Catalyst

At the outset, $[\gamma\text{-Fe}_2\text{O}_3@\text{HAp-Si}(\text{CH}_2)_3\text{Cl}@\text{DMIM}]$ MNPs were prepared by the reaction of 1,2-dimethylimidazole and $[\gamma\text{-Fe}_2\text{O}_3@\text{HAp-Si}(\text{CH}_2)_3\text{Cl}]$. In the next step, the prepared compound reacted with NaBF_4 to produce the desired $[\gamma\text{-Fe}_2\text{O}_3@\text{HAp-Si}(\text{CH}_2)_3\text{BF}_4@\text{DMIM}]$ MNPs (**Scheme 1**). The product was fully characterized by various spectroscopic, thermogravimetric and magnetic methods (**Fig. 1-6**).



Scheme 1. Synthesis of $[\gamma\text{-Fe}_2\text{O}_3\text{@HAp-Si}(\text{CH}_2)_3\text{BF}_4\text{@DMIM}]$ (5).

3.2. Characterization techniques

3.2.1. FT-IR

Functional groups of the prepared catalyst characterized by FT-IR spectrum are presented in **Fig. 1**. Stretching vibrations of hydroxyl group appeared at 3412 cm^{-1} . The

stretching vibration at 1639 cm^{-1} attributed to the carbon-nitrogen double bond. Fe-O in magnetite structure stretched at $443\text{--}634\text{ cm}^{-1}$. Shoulder at 1094 cm^{-1} is attributed to Si-O stretching and band at 1037 cm^{-1} is related to the P-O bond. Also, the O-P-O stretching related to the phosphate in the $\text{Ca}_5(\text{PO}_4)_3\text{OH}$ coating appeared at 566 and 602 cm^{-1} which is overlapping with Fe-O band [28, 29].

3.2.2. XRD

X-ray powder diffraction of the catalyst is presented in **Fig. 2**. As expected, all the diffraction peaks of magnetite (ICDD no. 39-1346) are exhibited in the XRD pattern confirming that the core of the prepared nanoparticles is made of magnetite.

3.2.3. EDX

Elemental analysis of the prepared catalyst (**Fig. 3**), confirmed the presence of boron (1.88 w%), carbon (8.37 w%), nitrogen (5.35 w%), oxygen (39.76 w%), Fluor (5.76 w%), silicon (0.62 w%), phosphorous (5.35 w%), calcium (11.66 w%) and iron (21.24 w%) in its structure.

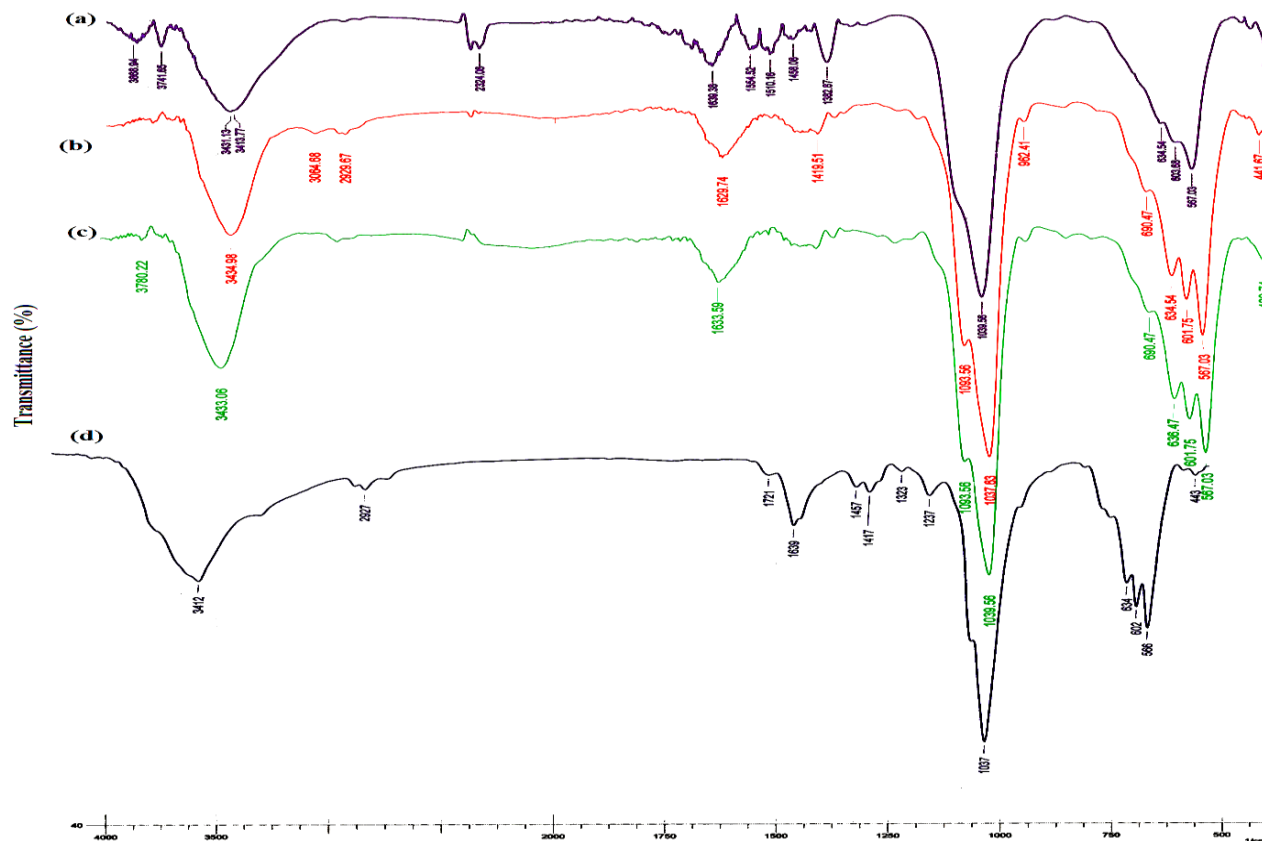


Fig. 1. FT-IR spectrum. (a) $[\gamma\text{-Fe}_2\text{O}_3\text{@HAp}]$, (b) $[\gamma\text{-Fe}_2\text{O}_3\text{@HAp-Si}(\text{CH}_2)_3\text{Cl}]$, (c) $[\gamma\text{-Fe}_2\text{O}_3\text{@HAp-Si}(\text{CH}_2)_3\text{Cl@DMIM}]$, (d) $[\gamma\text{-Fe}_2\text{O}_3\text{@HAp-Si}(\text{CH}_2)_3\text{BF}_4\text{@DMIM}]$.

3.2.4. SEM

Scanning electron microscopy of the catalyst can be seen in **Fig. 4a** which shows the size of 60-75 nm for the synthesized nanoparticles. It is measured as about 49 nm by FE-SEM (**Fig. 4b**).

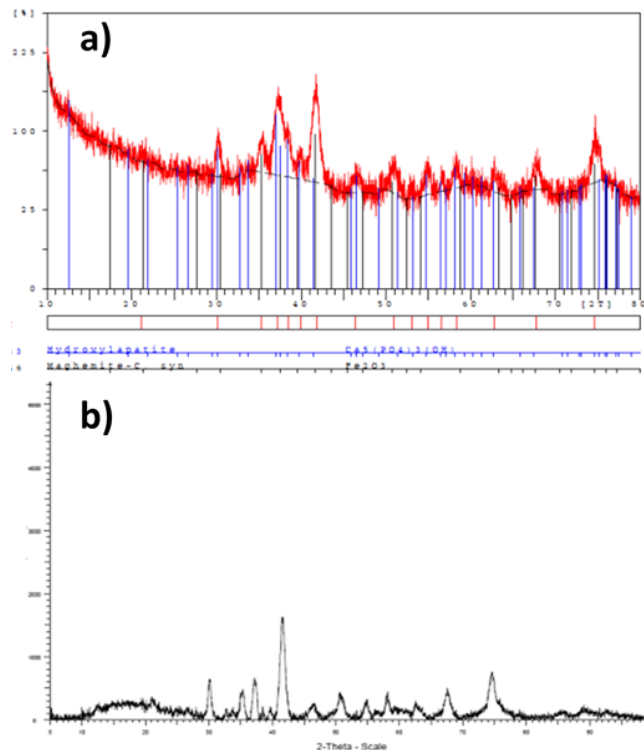


Fig. 2. XRD pattern of a) $[\gamma\text{-Fe}_2\text{O}_3\text{@HAP}]$, b) $[\gamma\text{-Fe}_2\text{O}_3\text{@HAP-Si}(\text{CH}_2)_3\text{BF}_4\text{@DMIM}]$ nanocatalyst

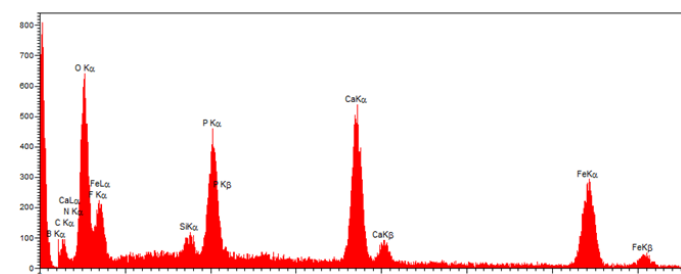


Fig. 3. EDX analysis.

3.2.5. TGA-DTG

Thermal Analyses of the catalyst are shown in **Fig. 5**, which were done from r.t to 600 °C. There are two significant weight loses; the first is related to dehydration ($t < 100$ °C) and the second is due to loss of organic molecules of the catalyst ($350 < t < 600$ °C).

3.2.6. VSM

To investigate the recoverability of the catalyst, its magnetic feature was evaluated via VSM analysis in a field swipping from -8000 - 8000 Oersted (**Fig. 6**). Analysis confirmed its super magnetic property (no

remanence, to ensure that particles are not agglomerated) with an M_s about 14.3 emu/g .

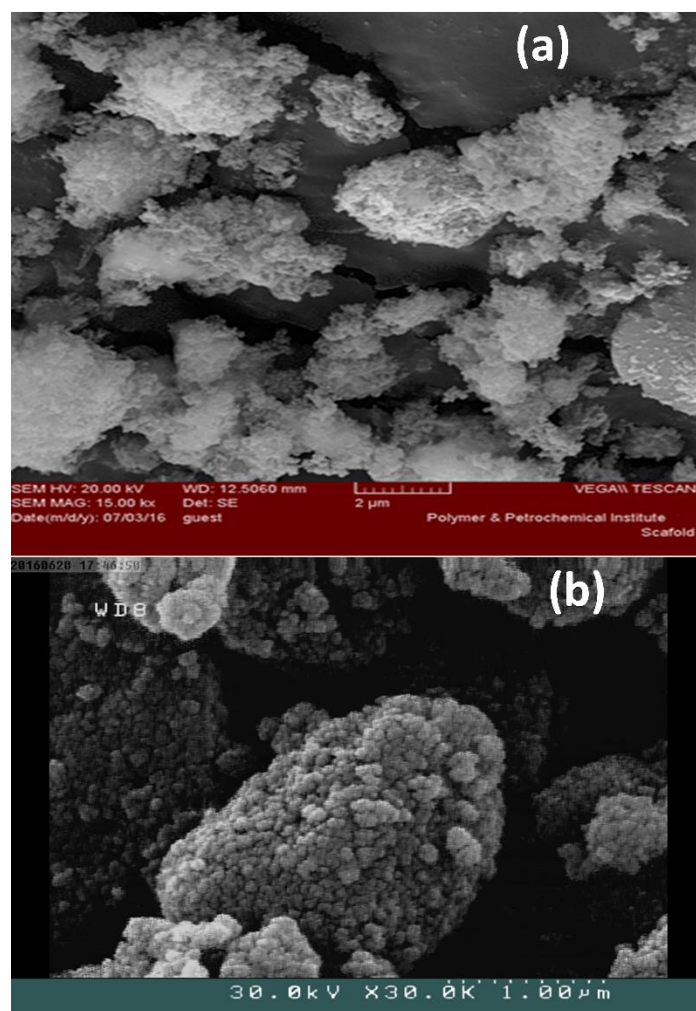


Fig. 4. a) SEM, b) FE-SEM images.

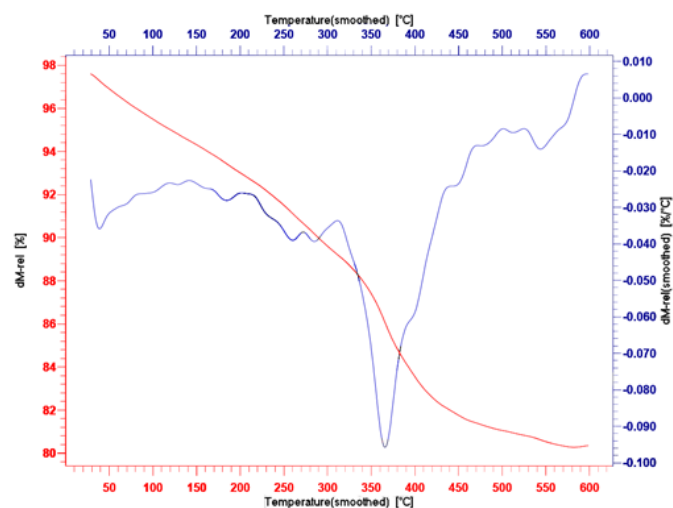


Fig. 5. TGA curves and DTG.

After characterization of the catalyst, we employed the synthesized nanocatalyst as catalyst for the synthesis of

chromene derivatives. Thus, one-pot three-component synthesis of 2-amino-4-(3-methylphenyl)-3-cyano-7,7-dimethyl-5-oxo-4H-5,6,7,8-tetrahydrobenzo-pyran (**11a**) by reaction of malononitrile, dimedone and 3-methylbenzaldehyde was used as a model reaction. The reaction mixture was heated in the presence of nanocatalyst **5** (0.02 g/mmol substrate) (**Scheme 2**). Different solvents were evaluated to obtain the optimal conditions among which EtOH showed the best result (**Table 1**, entry 3). Also it was observed that 0.02 g of catalyst/mmol of aldehyde in refluxing EtOH was the ideal amount of the catalyst in the reaction (**Table 2**).

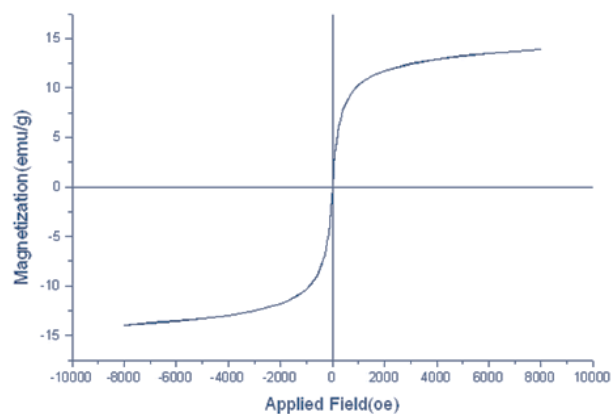
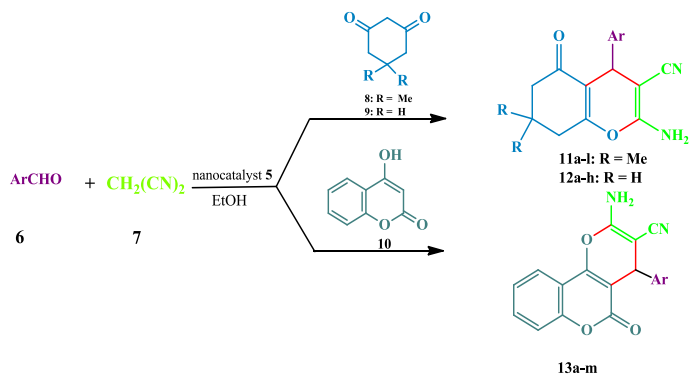


Fig. 6. VSM of the nanocatalyst.



Scheme 2. Synthesis of chromene derivatives using $[\gamma\text{-Fe}_2\text{O}_3@ \text{HAp-Si}(\text{CH}_2)_3\text{BF}_4@ \text{DMIM}]$ (**5**)

Table 1. Effect of solvent on synthesis of **11a** in the presence of $[\gamma\text{-Fe}_2\text{O}_3@ \text{HAp-Si}(\text{CH}_2)_3\text{BF}_4@ \text{DMIM}]$ MNPs.

Entry	Solvent	T (°C)	Time (min)	Yield (%) ^a
1	EtOH	40	95	47
2	EtOH	60	15	61
3	EtOH	80	15	95
4	H ₂ O	90	95	45
5	THF	60	--	25
6	Ethylene glycol	120	120	42
7	CH ₂ Cl ₂	40	60	55

^aIsolated yield.

Table 2. Optimization of the amount of $[\gamma\text{-Fe}_2\text{O}_3@ \text{HAp-Si}(\text{CH}_2)_3\text{BF}_4@ \text{DMIM}]$ MNPs for the synthesis of **11a**.

Entry	Amount of Cat. (g/mmol)	Time (min)	Yield (%) ^a
1	0.005	25	84
2	0.01	20	90
3	0.02	15	95
4	0.03	15	95

^aIsolated yield.

The efficacy of catalyst **5** in the synthesis of **11a** was compared with some other basic and acidic catalysts (**Table 3**). The results showed that using the synthesized catalyst a higher yield (95%) was obtained in shorter time (15 min).

Table 3. Comparison of different catalysts for the synthesis of **11a** in the presence of $[\gamma\text{-Fe}_2\text{O}_3@ \text{HAp-Si}(\text{CH}_2)_3\text{BF}_4@ \text{DMIM}]$ MNPs.

Entry	Catalyst ^b	Time (min)	Yield (%) ^a
1	--	180	60
2	NEt ₃	150	65
3	DBU	170	57
4	DABCO	160	60
5	AcOH	130	64
6	<i>p</i> -TSA	110	68
7	Fe ₃ O ₄	40	78
8	KHSO ₄	40	83
9	MnO ₂	45	66
10	CeO ₂	45	74
11	ZrO ₂	50	66
12	[bmim][PF ₆]	45	72
13	$[\gamma\text{-Fe}_2\text{O}_3@ \text{HAp}]$	25	80
14	$[\gamma\text{-Fe}_2\text{O}_3@ \text{HAp-Si}(\text{CH}_2)_3\text{Cl}@ \text{DMIM}]$	20	85
15	$[\gamma\text{-Fe}_2\text{O}_3@ \text{HAp-Si}(\text{CH}_2)_3\text{BF}_4@ \text{DMIM}]$	15	95

^aIsolated yield. ^bReaction conditions: catalyst (entries 2-12, 20 mol%; entries 13-15, 0.02 g/mmol substrate), EtOH (10 mL), 80 °C.

After optimization, a number of chromenes were prepared under these conditions (**Table 4**, **Fig.7**). Taking substituent effect into consideration showed that using both EWGs and EDGs resulted in excellent yields in the preparation of products **11-13** (90-97%). In both cases, as shown in **Scheme 3**, the catalyst prepares benzaldehyde for nucleophilic attack of malononitrile. By altering the substituent on benzaldehyde appreciable changes in the yield and the reaction time was not observed which could be attributed to the rate determining the step of the reaction. Also, in the present procedure TONs and TOFs in **Table 4** indicate high-

Table 4. Synthesis of chromone derivatives using $[\gamma\text{-Fe}_2\text{O}_3\text{@HAp-Si}(\text{CH}_2)_3\text{BF}_4\text{@DMIM}]\text{MNPs}$.

Entry	Ar	Product	Time (min)	Yield (%) ^a	TON	TOF(1/h)	M. P. (°C)	
							Found	Reported [Ref.]
1	3-MeC ₆ H ₄	11a	15	95	25	100	198-200	-
2	2-FC ₆ H ₄	11b	15	93	24	96	250-251	-
3	2-ClC ₆ H ₄	11c	13	95	25	114	213-215	214-215 [33]
4	2-MeOC ₆ H ₄	11d	10	96	25	147	202-204	-
5	3-O ₂ NC ₆ H ₄	11e	15	97	25	100	212-213	213 [33]
6	4-BrC ₆ H ₄	11f	15	95	25	100	202-203	201-203 [34]
7	4-FC ₆ H ₄	11g	15	94	25	100	192-193	191-193 [34]
8	4-MeOC ₆ H ₄	11h	15	93	24	96	197-199	198 [33]
9	4-MeC ₆ H ₄	11i	14	95	25	109	209-210	208-210 [32]
10	4-O ₂ NC ₆ H ₄	11j	15	97	25	100	179-180	178-180 [32]
11	C ₆ H ₅	11k	15	96	25	100	231-233	232-234 [32]
12	4-ClC ₆ H ₄	11l	14	95	25	109	215-217	213-215 [33]
13	2-MeOC ₆ H ₄	12a	15	91	24	96	193-194	-
14	2-BrC ₆ H ₄	12b	14	91	24	104	194-196	-
15	2-FC ₆ H ₄	12c	15	94	25	100	252-253	-
16	3-MeC ₆ H ₄	12d	15	92	24	96	220-221	-
17	4-HO-3-MeO-C ₆ H ₃	12e	20	91	24	73	239-241	-
18	3-O ₂ NC ₆ H ₄	12f	20	95	25	76	199-200	199-201 [34]
19	4-ClC ₆ H ₄	12g	15	96	25	100	223-224	223-225 [34]
20	4-MeOC ₆ H ₄	12h	15	94	25	100	190-193	191-193 [34]
21	C ₆ H ₅	13a	15	95	25	100	256-259	256-258 [32]
22	2,4-Cl ₂ C ₆ H ₃	13b	20	91	24	73	255-257	257-259 [36]
23	4-HOC ₆ H ₄	13c	17	90	24	86	260-261	258-260 [35]
24	3-BrC ₆ H ₄	13d	17	94	25	89	278-280	280-282 [34]
25	4-BrC ₆ H ₄	13e	15	95	25	100	248-249	249-251 [32]
26	3-ClC ₆ H ₄	13f	14	95	25	109	242-243	240-241 [18]
27	4-ClC ₆ H ₄	13g	14	93	24	104	258-260	257-259 [32]
28	3-O ₂ NC ₆ H ₄	13h	15	92	24	96	259-261	260-263 [35]
29	4-O ₂ NC ₆ H ₄	13i	15	96	25	100	257-259	258-260 [32]
30	2-MeOC ₆ H ₄	13j	14	94	25	109	231-233	233-235 [35]
31	3-MeOC ₆ H ₄	13k	14	93	24	104	242-244	240-243 [35]
32	4-MeC ₆ H ₄	13l	14	95	25	109	249-252	251-253 [32]
33	4-FC ₆ H ₄	13m	15	91	24	96	255-256	257-259 [34]

^aIsolated yield.

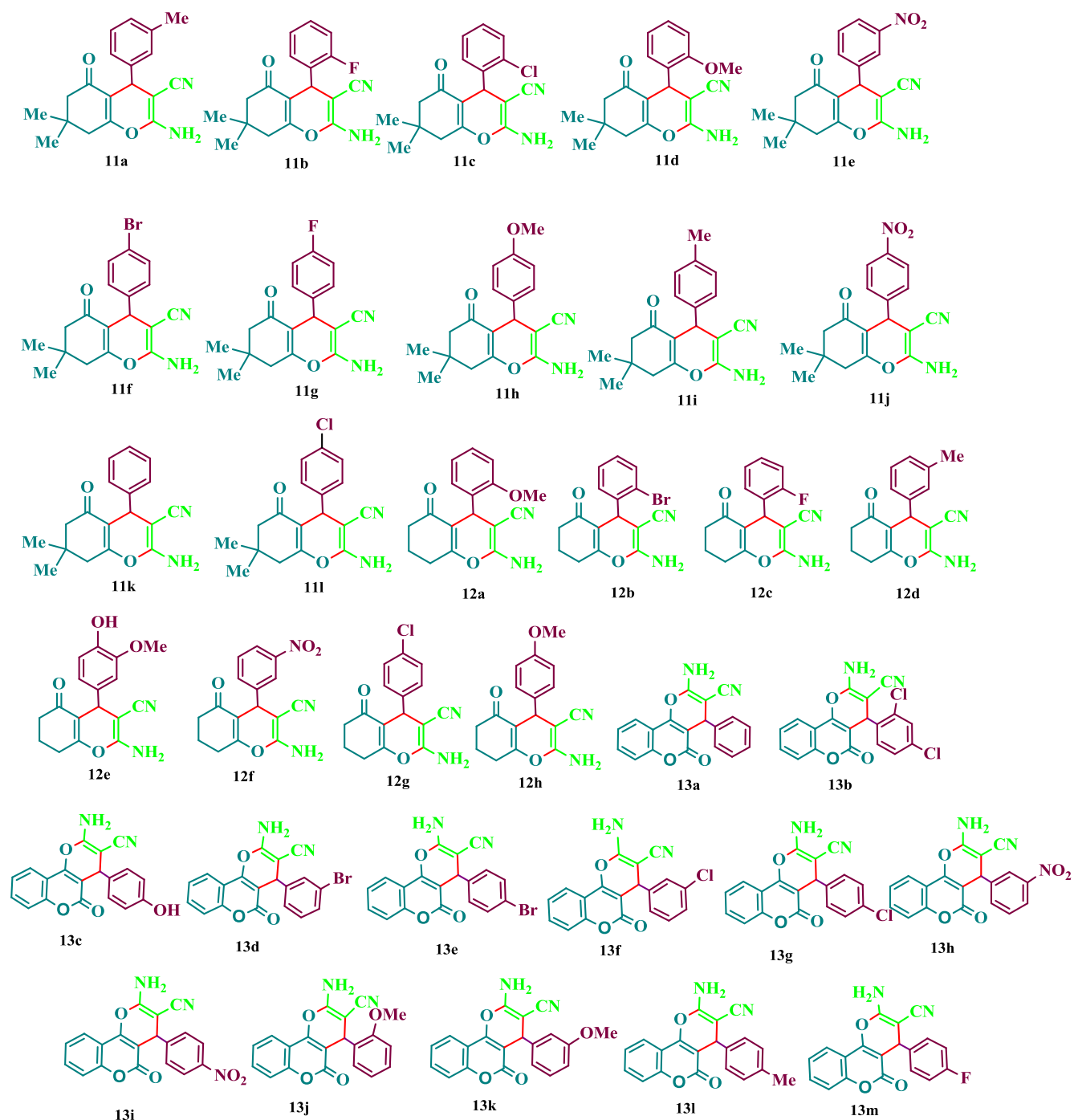


Fig. 7. The synthesized chromene derivatives (11-13).

-activity of the synthesized MNPs. All the synthesized products (**Fig. 7**) were characterized FT-IR, ^1H NMR and ^{13}C NMR analyses.

The recoverability of the catalyst **5** was also investigated. To this end, after magnetic decanting of the catalyst from the reaction mixture and washing with EtOH, it was dried under reduced pressure and reused in the same reaction. No meaningful decreasing of activity was observed after eight successive reactions (**Fig. 8**).

The proposed reaction pathway is shown in **Scheme 3**. As it is shown, the nucleophile attacks the aldehyde after its activation by the catalyst. After a conjugate addition and an intramolecular annulation, the intermediate tautomerizes to the desired product.

A comparison of this method with some reported ones are presented in **Table 5**. It is clear from the results that the present protocol has higher efficiency which led to products in higher yields and lower reaction times.

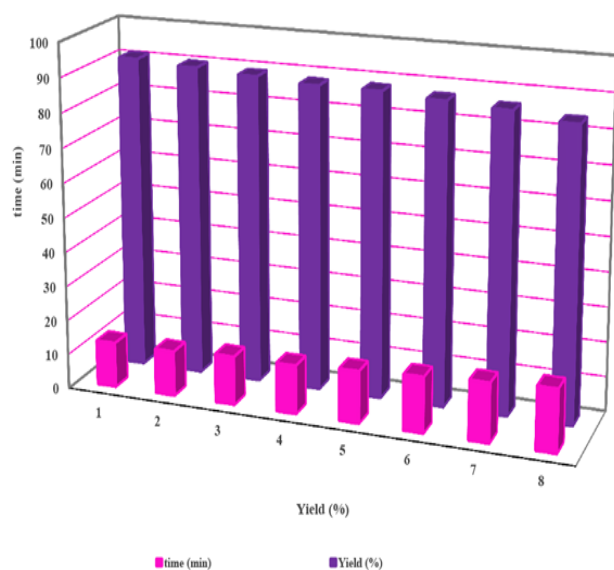


Fig.8. Reusability of the nanocatalyst in synthesis of chromene **11a**.

Table 5. Comparison of the catalytic performance of $[\gamma\text{-Fe}_2\text{O}_3@ \text{HAp-Si}(\text{CH}_2)_3\text{BF}_4@ \text{DMIM}] \text{MNPs}$ with the previous reports in synthesis of **11i**.

Entry	Catalyst	Solvent	Time (min)/T (°C)	Yield (%)	Ref
1	CuO nanobelts	water: EtOH (70:30)	50/25	90	[33]
2	Sodium hydroxide	EtOH	240/reflux	66	[37]
3	<i>L</i> -proline	EtOH	115/reflux	90	[38]
4	Silica-bonded DABCO	EtOH	30/25	93	[39]
5	KCC-1	EtOH	45/reflux	85	[21]
6	KCC-1-NH ₂	EtOH	35/reflux	88	[22]
7	KCC-1-NH-CS ₂	EtOH	25/reflux	92	[21]
8	$[\gamma\text{-Fe}_2\text{O}_3@ \text{HAp-Si}(\text{CH}_2)_3\text{BF}_4@ \text{DMIM}]$	EtOH	14/reflux	95	This work

4. Conclusions

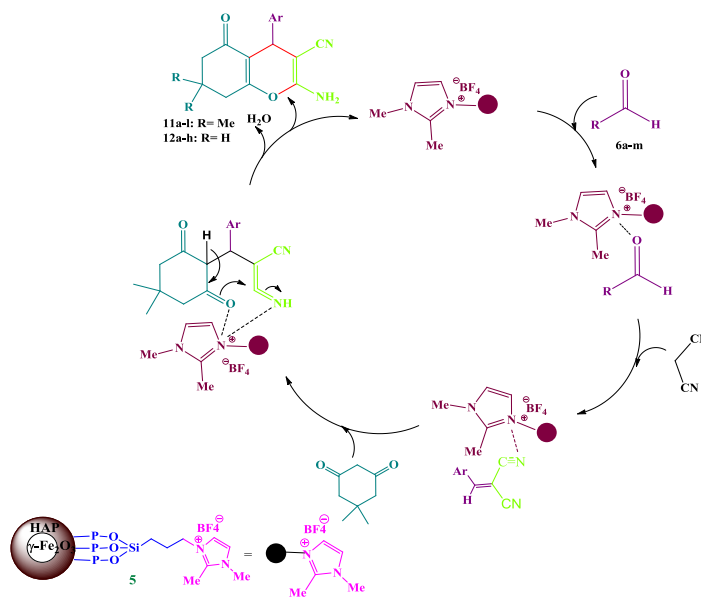
In conclusion, we report the synthesis of a variety of chromenes through a three-component reaction in the presence of catalytic amount of an imidazolium based ionic liquid embedded on hydroxyapatite encapsulated maghemite $[\gamma\text{-Fe}_2\text{O}_3@ \text{HAp-Si}(\text{CH}_2)_3\text{BF}_4@ \text{DMIM}] \text{MNPs}$ in 10-20 min and high yield (90-97%). This novel protocol has various advantages such as short reaction times, simple work-up, mild reaction conditions and magnetic recoverability of the catalyst. Thus, it could be considered as a suitable method in the synthetic organic chemistry to the synthesis of chromene derivatives.

Acknowledgements

The authors are grateful to the Research Council of Islamic Azad University, Rasht Branch for partial support of this project.

References

[1] R. Pratap, V. Ji Ram, Chem. Rev. 114 (2014) 10476-10526.



Scheme 3. Proposed mechanism for the synthesis of chromene derivatives using $[\gamma\text{-Fe}_2\text{O}_3@ \text{HAp-Si}(\text{CH}_2)_3\text{BF}_4@ \text{DMIM}]$ (**5**)

- [2] M. Gold, Y. Mujahid, Kh. Ahmed, H. Kostrhunova, J. Kasparkova, V. Brabec, B. Biersack and R. Schobert, J. Biol. Inorg. Chem. 24 (2019) 647-657.
- [3] K. Y. Lum, A. R. Carroll, M. G. Ekins, S. Read, Z. Haq, I. Tietjen, J. S. John and R. A. Davis, Mar. Drugs. 17 (2019) 26-34.
- [4] J. Chen, J. Cho, T. Hwang and I. Chen, J. Nat. Prod. 71 (2008) 71-75.
- [5] W. Gregor, G. Grabner, C. Adelwohrer, T. Rosenau and L. Gille, J. Org. Chem. 70 (2005) 3472-3483.
- [6] C. Bruhlmann, F. Ooms, P. Carrupt, B. Testa, M. Catto, F. Leonetti, C. Altomare and A. Cartti, J. Med. Chem. 44 (2001) 3195-3198.
- [7] A. Aminkhani, M. Talati, R. Sharifi, F. Chalabian and F. Katouzian, J. Heterocycl. Chem. 56 (2019) 1812-1819.
- [8] N. D. Thanh, D. Son Hai, V. Th. Ngoc Bich, Ph. Th. Thu Hien, N. Th. Ky. Duyen, N. Th. Mai, T. Th. Dung, V. N. Toan, H. Th. Kim Van, L. H. Dang, D. N. Toan and T. Th. Thanh Van, Eur. J. Med. Chem. 167 (2019) 454-471.
- [9] F. F. Alblewi, R. M. Okasha, Z. M. Hritani, H. M. Mohamed, M. A.A. El-Nassag, A. H. Halawa, A. Mora, A. M. Fouda, M. A. Assiri, Al-A. M. Al-Dies, T. H. Afifi and A. M. El-Agrody, Bioorg. Chem. 87 (2019) 560-571.

- [10] O. J. Jesumoroti, D. Faridoon, M. Mnkandhla, H. C. H. Isaacs and R. Klein, *Med. Chem. Commun.* 10 (2019) 80-88.
- [11] A. Yu. Sidorenko, A. V. Kravtsova, A. Aho, I. Heinmaa, J. Wärnå, H. Pazniak, K. P. Volcho, N. F. Salakhutdinov, D. Yu. Murzin and V.E. Agabekov, *J. Catal.* 374 (2019) 360-377.
- [12] A. Smuszkiwicz, J. L'opez-Sanz, I. Sobczak, R. M. Martin-Aranda, M. Ziolk and E. Perez-Mayoral, *Catal. Today.* 325 (2019) 47-52.
- [13] J. Balou, M. A. Khalilzadeh and D. Zareyee, *Sci. Rep.* 9 (2019) 3605-3613.
- [14] Y. Pourshojaei, F. Zolala, Kh. Eskandari, M. Talebi, L. Morsali, M. Amiri, A. Khodadadi, R. Shamsimeymandi, E. Faghieh-Mirzaei, A. Asadipour, *J. Nanosci. Nanotechnol.* 20 (2020) 3206-3216.
- [15] J. Albadi, H. Samimi, A. R. Momeni, *Chem. Methodol.* 4 (2020) 565-571.
- [16] R. Mohammadipour, A. Bamoniri, B. B. F. Mirjalili, *Sci. Iran.* 27 (2020) 1216-1225.
- [17] A. Rimus Liandi, R. Tri Yunarti, M. Fajri Nurmawan, A. Herry Cahayana, *Mater Today* 22 (2020) 193-198.
- [18] N. Monadi, H. Davoodi, M. Aghajani, *React. Kinet. Mech. Catal.* 129 (2020) 659-677.
- [19] M. A. Bodaghifard, Z. Mozaffari, Z. Faraki, *Iran. J. Catal.* 10 (2) (2020) 101-110.
- [20] M. Pourghasemi, F. Shirini, M. Alinia-Asli, M. A. Rezvani, *J. Nanosci. Nanotechnol.* 20 (2020) 973-982.
- [21] M. Anvari Gharabaghlo, N. Shadjou, A. Poursattar Marjani, *Appl. Organomet. Chem.* 2020; e 5868.
- [22] H. Naeimi, S. Mohammadi, *ChemistrySelect* 5 (2020) 2627-2633.
- [23] A. R. Moosavi-Zare, H. Afshar-Hezarkhani, *Iran. J. Catal.* 10 (2) (2020) 119-126.
- [24] P. Jahanshahi, M. Mamaghani, F. Haghbin, R. Hosseini and M. Rassa, *J. Mol. Struct.* 1155 (2018) 520-529.
- [25] M. Mohsenimehr, M. Mamaghani, F. Shirini, M. Sheykhani, S. Abbaspour and L.S. Sabet, *J. Chem. Sci.* 127 (2015) 1895-1904.
- [26] M. Mamaghani, F. Shirini, M. Sheykhani and M. Mohsenimehr, *RSC Adv.* 5 (2015) 44524-44529.
- [27] P. Farokhian, M. Mamaghani, N. O. Mahmoodi, K. Tabatabaeian and A. Fallah Shojaie, *J. Chem. Res.* 43 (2019) 135-139.
- [28] M. Sheykhani, L. Ma'mani, A. Ebrahimi and A. Heydari, *J. Mol. Catal. A: Chem.* 335 (2011) 253-261.
- [29] L. Ma'mani, M. Sheykhani, A. Heydari, M. Faraji and Y. Yamini, *Appl. Catal. A.* 377 (2010) 64-69.
- [30] Mamaghani, M., Shirini, F., Bassereh, E., Nia, R. H., *J. Saudi Chem. Soc.* 20 (5) (2016) 570-576.
- [31] a) N. Lakshmi, P. Thirumurugan, K. M. Noorulla and P. T. Perumal, *Bioorg. Med. Chem. Lett.* 20 (2010) 5054-5061. b) P. Borah, P. S. Naidu, S. Majumder and P. Bhuyan, *J. Mol. Divers.*, 2014, 18, 759-767.
- [32] A. Hallaoui, S. Chehab, B. Malek, O. Zimou, T. Ghailane, S. Boukhris, A. Souizi and R. Ghailane, *ChemistrySelect* 4 (2019) 3062-3070.
- [33] A. Mulik, P. Hegade, S. Mulik and M. Deshmukh, *Res. Chem. Intermediat.* 45 (2019) 5641-5647.
- [34] M. Mashhadinezhad, M. Mamaghani, M. Rassa and F. Shirini, *ChemistrySelect* 4 (2019) 4920-4932.
- [35] W. Ma, A. Gh. Ebadi, M. Shahbazi Sabil, R. Javahershenas and G. Jimenez, *RSC Adv.* 9 (2019) 12801-12812.
- [36] Gh. Mohammadi Ziarani, A. Badiei, M. Azizi and P. Zarabadi, *Iran. J. Chem. Chem. Eng.* 30 (2) (2011) 59-65.
- [37] P. Mukherjee and R. A. Das, *J. Org. Chem.* 81(13) (2016) 5513-5524.
- [38] A. Ovchinnikova and A. N. Andin, *Russ. J. Org. Chem.* 49 (2013) 1067-1071.
- [39] A. Hasaninejad, N. Golzar, M. Beyrati, A. Zare, and M. M. Doroodmand, *J. Mol. Catal. A: Chem.* 372 (2013) 137-150.